Title

Cellular Uptake Evaluation of Amphiphilic Polymer Assemblies: Importance of Interplay between Pharmacological and Genetic Approaches.

Journal

Biomacromolecules, 20(12)

Authors

He, Huan

Liu, Hongxu

Thayumanavan, S

et al.

Publication Date

2019-12-09

DOI

10.1021/acs.biomac.9b01073

Peer reviewed

HHS Public Access

Author manuscript

Biomacromolecules. Author manuscript; available in PMC 2020 December 09.

Published in final edited form as:

Biomacromolecules. 2019 December 09; 20(12): 4407–4418. doi:10.1021/acs.biomac.9b01073.

Cellular Uptake Evaluation of Amphiphilic Polymer Assemblies: Importance of Interplay between Pharmacological and Genetic Approaches

Ziwen Jiang[†], **Huan He**[†], **Hongxu Liu**[†], **S. Thayumanavan**[†,‡,§]

[†]Department of Chemistry, University of Massachusetts Amherst, Massachusetts 01003, United States

[‡]Molecular and Cellular Biology Program, University of Massachusetts Amherst, Massachusetts 01003, United States

[§]Center for Bioactive Delivery at the Institute for Applied Life Sciences, University of Massachusetts Amherst, Massachusetts 01003, United States

Abstract

Understanding the cellular uptake mechanism of materials is of fundamental importance that would be beneficial for materials design with enhanced biological functions. Herein, we report the interplay of pharmacological and genetic approaches to minimize the possible misinterpretation on cellular uptake mechanism. A library of amphiphilic polymers was used as a model system to evaluate the reliability of such methodological interplay. To probe the cellular uptake of amphiphilic polymers, we utilized an orthogonal end-group labelling strategy to conjugate one fluorescent molecule on each polymer chain. The results from the methodological interplay with these labelled polymers revealed the off-target effects of dynasore, a well-known dynamin inhibitor. Instead of dynamin, actin was found to be an essential cellular component during the cellular uptake of these amphiphilic polymers. Our study demonstrates the importance of interplaying pharmacological and genetic approaches when evaluating the endocytic mechanism of functional materials, providing insights on understanding the cellular uptake of future therapeutic materials.

Graphical Abstract

Author Contributions

Z.J. and S.T. conceived the project. Z.J. conducted all the experiments and analyzed the results, with the help from H. H. and H. L. for synthesis. Z.J. and S.T. wrote the manuscript. All authors reviewed the manuscript.

Supporting Information

The Supporting Information is available.

Supplementary figures and tables, Characterization of each polymer, and Spectral data.

The authors declare no competing interest.

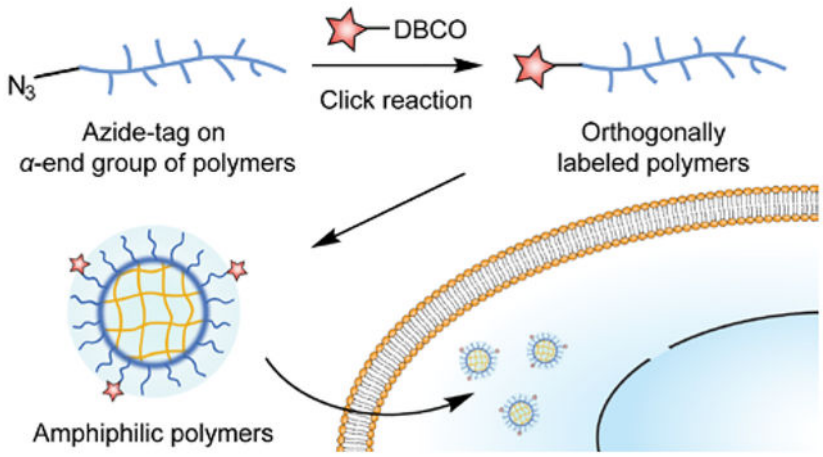

Introduction

Passing across the cell membrane is one of the preliminary processes for therapeutic materials to initiate their intracellular biological functions.[1–3] An efficient cellular entry of therapeutic materials is therefore a fundamental step to achieve high biological efficacy. Thus, understanding the cellular internalization mechanism would provide rational basis for materials design, tuning their interaction with the cell membrane, and improving their cellular uptake efficiency.[4–6]

The most commonly used method to probe cellular uptake mechanism is the pharmacological approach, where an inhibitor is applied to investigate the endocytic pathway of interest.[7] However, several representative inhibitors of endocytic pathways could concurrently affect multiple pathways. The off-target effects of these inhibitors typically result from either non-specific interference with different cellular components, or disruption of a cellular component that involves in multiple biological pathways.[8] Alternatively, genetic approaches are introduced through expressing the mutant forms of the target protein or downregulating the protein that is responsible for one endocytic pathway.[9] Like pharmacological approaches, alteration of endogenous proteins can also lead to the regulation of other endocytic pathways.[8] In fact, it is hard to conclude the endocytic pathway for a certain nanomaterial exclusively based on one approach.[10, 11] The interplay of pharmacological and genetic approaches is expected to minimize misleading interpretations on cellular uptake mechanism.

Here we evaluate the cellular uptake of amphiphilic polymers as a model system to investigate the interplay of pharmacological and genetic approaches. Amphiphilic polymers are broadly used as drug carriers for the development of nanomedicines.[12, 13] The amphiphilic feature allows these carriers to accommodate a large range of therapeutic cargos, including hydrophobic small molecules[14, 15] and hydrophilic biomacromolecules.[16, 17] To probe the cellular uptake and intracellular trafficking of amphiphilic polymers, utilizing fluorescence is a straightforward way to evaluate in live cells. Fluorescent molecules can be non-covalently encapsulated by the hydrophobic moieties within the polymers,[18] or covalently attached onto the polymers.[19] However, the non-covalent strategy

is in fact tracking the encapsulated fluorescent molecules, rather than directly monitoring polymers. Possible fluorophore leakage during the uptake process will generate false signals for the localization of polymers. In contrast, covalently attaching fluorophores on polymers avoids such disadvantage.[20, 21]

Strategies to covalently attach fluorophores are mainly designed for incorporation on the side chain of polymers, where a small percentage functionalization is targeted.[22, 23] Such a strategy results in significant dispersity in the number of fluorophores on each polymer chain. Since typical fluorescent molecules are quite hydrophobic, multi-fluorophore labeling on an amphiphilic polymer chain could affect the hydrophilic-lipophilic balance of the polymer and induce unnecessary complications during the cellular uptake evaluation. In this study, we introduce an orthogonal labeling strategy[24] via covalently tagging the end group of each polymer chain. Previous studies have demonstrated the end group labeling strategy based on a pentafluorophenol (PFP) ester-terminated polymer.[25] However, the chain transfer reagent and initiator for the PFP-based strategy were found to be labile in protic solvent at elevated temperatures.[26] Our strategy ensures single fluorophore labeling per polymer chain through azide-alkyne click reaction,[27] precisely controlling the attachment of fluorophore label. Next, by tracking the labeled fluorophore, the cellular uptake mechanism of an amphiphilic polymer analog was investigated by both pharmacological and genetic approaches. We report that the methodological interplay on deciphering endocytic mechanisms has minimized the misinterpretation that can be generated by one methodology alone, improving our understanding on the cellular entry of functional materials.

Experimental Section

General methods.

Materials and reagents were purchased from commercial sources without further purification. ^{1}H NMR, ^{13}C NMR, ^{19}F NMR, and ^{31}P NMR spectrum were acquired from either a Bruker AdvanceIII 400 NMR spectrometer or a Bruker AvanceIII 500 NMR spectrometer. Mass spectrometry was conducted on a Bruker MicrOTOF ESI-TOF mass spectrometer. Gel permeation chromatography (GPC) was conducted on an Agilent 1260 LC using tetrahydrofuran as the eluent. Molecular weights are versus polystyrene standards. The GPC using trifluoroethanol as the eluent was conducted on an Agilent 1200 series HPLC system, using polymethylmethacrylate standards for molecular weight calculation. Dynamic light scattering and zeta potential measurement were carried out on a Malvern Zetasizer Nano ZS. Confocal microscopy images were obtained from a Nikon fluorescence microscope either equipped with a Yokogawa spinning disk or a spectral detector unit. Flow cytometry experiments were conducted on a ThermoFisher Attune NxT flow cytometer. The infrared spectra were collected on a Bruker Alpha FT-IR Spectrometer with a spectral range from 3500 cm^{-1} to 400 cm^{-1}. Thermogravimetric analysis was performed under N_2 flow from room temperature to 600 °C using a TA Instrument Q50 thermogravimetric analyzer.

Synthesis of chain transfer agent, radical initiator, monomers, and polymers.

The detailed synthetic procedures are provided in Section 2.1. and 2.2. of the Supporting Information. Specifically, the synthesis of the chain transfer agent (**Az-CTAP**, Figure 1), the

radical initiator (**Az-ACVA**, Figure 1), and monomers for the reversible addition–fragmentation chain transfer (RAFT) polymerization are summarized (Figure SP1~SP11). RAFT polymerization of the polymers with different surface charge are also summarized with structural characterization results (Figure S1, SP12~SP20).

End-group labeling on the polymers *via* copper-free click chemistry.

Polymers and DBCO-Cy3 (Lumiprobe, Cat# E10F0, 1.05 equiv. vs. the azido-end-group on the polymer) were dissolved in trifluoroethanol (2 mL) and stirred at room temperature for 24 hours. The solvent was evaporated and the mixture was purified by gel permeation chromatography over SorbaDex 20-LH gel filtration matrix (Cat# 801009). Details of eluent are available in in Section 2.3. of the Supporting Information. The high-molecular-weight fraction was respectively collected and dried under vacuum (Figure S3).

Preparation of the amphiphilic polymer stock solution.

Amphiphilic polymer was first dissolved in organic solvent (details in the Section 2.4. of the Supporting Information). Deionized water was added dropwise into the organic solution of amphiphilic polymers while stirring. The mixture was continuously stirred at room temperature for 2 hours. Subsequently, a calculated amount of dithiothreitol stock solution was added into the mixture to crosslink ~20% pyridine disulfide unit. After stirring for overnight, the mixture was purified and concentrated with deionized water using Amicon centrifugal filters with 3 k MWCO.

Cellular uptake of amphiphilic polymers in the presence of pharmacological inhibitors.

A certain number of cells of interest were cultured in a 96-well plate for 24 hours prior to the experiment. For inhibiting different endocytic pathways, cells were cultured for 1 hour in the growth medium containing the inhibitor. Subsequently, in the presence of inhibitors, the cells were incubated with Cy3-labeled amphiphilic polymers that spiked into the medium for additional 3 hours. Note that the incubation time length for actin inhibitors is different from the rest of the inhibitors involved. Details are available in the Section 2.5., 2.6., 2.7., and 2.10. of the Supporting Information. After washing the cells with cold PBS, the fluorescence intensity of Cy3 within the cells was measured using flow cytometry with an excitation wavelength of 561 nm. For the positive control, cells were cultured in the growth medium for 1 hour and incubated with Cy3-labelled polymers for another 3 hours. For the blank group, cells were cultured in the growth medium for 4 hours. After subtracting the fluorescence signal from the blank group, Cy3 fluorescence of the positive control group was normalized as 100%.

Dynamin-2 knockdown in DNM2-GFP SK-MEL-2 cells.

The SK-MEL-2 cells with GFP tagged on one endogenous DNM2 allele[28] were provided by Dr. David G. Drubin (University of California, Berkeley). Lipofectamine RNAiMAX (ThermoFisher, Cat# 13778030) was used to transfect the siRNA of dynamin-2 (siDNM2, ThermoFisher, Cat# S4212) into SK-MEL-2 cells. The sequence of siDNM2 is 5′-ACAUCAACACGAACCAUGA-3′. Lipofectamine RNAiMAX and siDNM2 were complexed for transfection based on the ThermoFisher manual. Details are available in the

Section 2.8. of the Supporting Information. The lipid-RNA complex containing Opti-MEM was added into each well and incubated for 48 hours or 72 hours. After washing with phosphate buffer saline, the siDNM2-treated SK-MEL-2 cells are ready to be further evaluated for the cellular uptake of polymers.

Results and Discussion

Orthogonal end-group labeling of amphiphilic polymers

We designed an end-group labelling strategy to conjugate a fluorophore on amphiphilic polymers, allowing us to track these polymers via fluorescence during their cellular uptake process. The orthogonal end-group labelling strategy for amphiphilic polymers was designed based on the mechanism of reversible addition-fragmentation chain transfer (RAFT) polymerization.[29] RAFT polymerization requires a radical initiator to start the propagation and a chain transfer agent to control the yielded polymers with low dispersity (*Đ*).[30] We chose the azido-derivative of 4-cyano-4-(phenylcarbonothioylthio)pentanoic acid (Az-CTAP, Figure 1a)[31] as the chain transfer reagent. Previous studies have shown that chemical modifications on the carboxylic acid end of CTAP do not affect its fragmentation ability during polymerization,[32–34] allowing the orthogonal end-group functionalization on the polymer. Meanwhile, we synthesized the azido-derivative of 4,4'-azobis(4-cyanovaleric acid) (Az-ACVA, Figure 1a) as the radical initiator, ensuring that the minor products originated from initiator fragments during RAFT polymerization are also functionalized with an azido group. Next, we selected a library of methacrylate monomers to build up the hydrophilic moieties of the amphiphilic polymers. Structural variations in these hydrophilic monomers allow us to vary the surface charge of the resultant polymer. The hydrophobic moieties were based on pyridyl disulfide ethyl methacrylate. The library of random copolymers was synthesized by RAFT polymerization (Figure 1b).

The library of amphiphilic polymers includes an oligo(ethylene glycol)-based charge neutral polymer (**PEG**), a quaternary amine-based positively charged polymer (**POS**), a sulfonate-based negatively charged polymer (**NEG**), and a phosphorylcholine-based zwitterionic polymer (**MPC**). During the cellular uptake mechanism evaluation, the surface charge difference is designed to provide a parametric variation to explore the interplay between pharmacological and genetic approaches (Figure 1c). It should be noted that we installed a portion of oligo(ethylene glycol)-based moieties in **POS** and **NEG** polymers to control the hydrodynamic diameter of the polymers within 10-nm range (Figure 1c). The size range allows ultimate *in vivo* renal clearance of these amphiphilic polymers.[35] After adding 10 mol% (vs. PDS units) of dithiothreitol to form the polymeric assemblies, the library of polymers is generally biocompatible at a concentration of 0.25 $mg \cdot mL^{-1}$ in HeLa cells (Figure 1d, S2). Next, to evaluate the cellular uptake of the amphiphilic polymers, the azido-containing amphiphilic polymers were labelled with dibenzocyclooctyne-Cy3 (DBCO-Cy3) via copper-free click reaction (Figure 1e, S3~S5).[36]

Dynasore significantly inhibits the cellular uptake of amphiphilic polymers

After confirming that the cellular uptake of amphiphilic polymers is through active transport (Figure 2a),[37, 38] we next investigated the effect of representative pharmacological inhibitors

on the cellular uptake of amphiphilic polymers. Five inhibitors were employed to understand the process, i.e. endocytic pathway. Amiloride interferes macropinocytosis via inhibiting the Na^+/H^+ exchange.[39] Methyl-β-cyclodextrin (MβCD) depletes plasma membrane cholesterol, an essential molecule for lipid raft/caveolae-mediated endocytosis.[40] Chlorpromazine causes a loss of clathrin on cell surface, thus inhibiting clathrin-mediated endocytosis.[41] Dynasore is traditionally known as an inhibitor for dynamins,[42] a class of GTPases that play an important role in membrane fission during clathrin-mediated endocytosis. Additionally, fucoidan blocks scavenger receptor-mediated endocytosis, as negatively charged macromolecules can be recognized by scavenger receptors.[43] The cellular uptake of amphiphilic polymers was compared in presence of the above inhibitors, respectively in six different type of mammalian cells.

Surface charge in general did not play a unique role in determining the endocytic pathway of amphiphilic polymers, indicating that amphiphilic polymers with different surface charge in our study enter cell through similar pathways (Figure 2b, Figure S6). Instead, the uptake of polymers was majorly affected by the choice of pharmacological inhibitors. MβCD and fucoidan showed negligible effect on the cellular uptake of amphiphilic polymers, indicating that lipid raft/caveolae- and scavenger receptor-mediated endocytosis is barely involved. Moderate reduction of cellular uptake was observed when treating cells with amiloride, indicating that macropinocytosis is contributing to the uptake of these polymers. The most significant reduction in cellular uptake was induced by dynasore treatment, while treatment with chlorpromazine caused only minor reduction in the cellular uptake of polymers. The screening reveals that clathrin-mediated endocytosis and macropinocytosis are majorly contributing to the cellular uptake of these amphiphilic polymers. The effect of dynasore on polymer uptake implies an important role of dynamin during endocytosis. The presence of fetal bovine serum (2%) did not alter the effect of dynasore during the cellular uptake of polymers (Figure S7). We further confirmed the effect of dynasore by its dose-dependent effect on the uptake of polymers (Figure 2c,e), as well as using Dyngo-4a, a more potent structural analog of dynasore (Figure 2d, S8).[44]

Cellular uptake of amphiphilic polymers did not decrease after dynamin depletion

Since the dynasore analog is traditionally known as a GTPase inhibitor that rapidly inhibits dynamin activity,[42, 44] we were interested in exploring the role of dynamin using genetic approaches during the endocytosis of amphiphilic polymers. Among all the dynamin isoforms, dynamin-2 is ubiquitously expressed in most cell types.[45] We utilized a SK-MEL-2 cell line in which one endogenous DNM2 allele was tagged with GFP,[28] correlating the expression of dynamin-2 to the intensity of GFP. Next, we used an siRNA for DNM2 (siDNM2) to knock down dynamin-2 in DNM2-GFP SK-MEL-2 cells, with the control group that transfected with scrambled siRNA (siScram) (Figure 3a,b). Subsequently, we evaluated the uptake of amphiphilic polymers in these dynamin-2 deficient cells. Surprisingly, comparing to the control group, the uptake amount of different amphiphilic polymers all increased in the dynamin-2 deficient SK-MEL-2 cells (Figure 3c,d). Previous studies have shown that dynamin-2 knockdown in mouse embryo fibroblasts resulted in the accumulation of F-actin,[46] possibly leading to the increase in the cellular uptake of polymers (further analysis on the contribution of actin is provided later in the article). Moreover, the

uptake of different polymers significantly decreased upon dynasore treatment in both the dynamin-2-deficient group and the control group. These results indicate that dynasore is not dominantly affecting the activity of dynamin-2, as the decrease of dynamin-2 level unexpectedly increased the cellular uptake of amphiphilic polymers (Figure 3, S9).

Although reducing dynamin-2 did not decrease the uptake of amphiphilic polymers, the role of remaining dynamin-2 and other dynamin isoforms is unknown. Thus, we evaluated the uptake of the polymers using dynamin triple knockout cells (Details are available in the Section 2.9. of the Supporting Information). Conditional dynamin triple knockout (TKO) mouse embryo fibroblasts[46] were generated from 4-hydroxytamoxifen (OHT)-inducible Cre recombinase transgenic mice with floxed dynamin alleles (provided as a gift by Dr. De Camilli). In a previous report, all the three isoforms of dynamin (dynamin-1, -2, -3) were confirmed to be depleted with OHT treatment.[47] Similar to the dynamin-2-deficient cells, the cellular uptake of amphiphilic polymers increased in dynamin-depleted cells (Figure 4a), indicating that all the isoforms of dynamin are not contributing to the uptake of amphiphilic polymers. Moreover, treatment cells with dynasore, amiloride, or ATP-depletion conditions respectively caused similar effect on the uptake of polymers regardless of the presence of cellular dynamins (Figure 4b,c, S10), confirming that dynamin is not an influential factor during the cellular uptake of amphiphilic polymers. So far, the results from genetic approach do not support the results from the pharmacological approach, *i.e.* dynasore treatment.

Off-target effects of dynasore on the cellular uptake of amphiphilic polymers

The results on dynamin activity from pharmacological and genetic approaches suggests possible off-target effects of dynasore. Revisiting the pharmacological approach for dynamin will be helpful to elucidate the role of dynamin during the endocytosis of amphiphilic polymers. Dynamin inhibitors have been developed to target a different active site or domain of the protein (Figure 5a). For example, both MiTMAB and OcTMAB target at the pleckstrin homology domain of dynamins.[48] The Dynole analog bind with an allosteric site of the GTPase domain.[49] We compared the cellular uptake of polymers in presence of OcTMAB or Dynole 34–2 (Figure 5b). However, their level of uptake suppression is not comparable to the effect of the dynasore analogs. Till now, we can confirm that dynamin is not as significantly involved as dynasore-treatment indicated during the endocytosis of amphiphilic polymers. Therefore, the dynasore analogs may have caused such significant decrease in the polymer uptake through its off-target effects on other cellular components.

Based on reported off-target effects of dynasore on cellular components,[50] we inspected each of these off-target effects by using another pharmacological inhibitor that targets the same cellular component (Figure 5a). Dynasore also affects the activity of mitochondrial dynamins[42] and vacuolar-type H^+-ATPase (V-ATPase).[51, 52] Mdivi-1 is a cell permeable inhibitor for mitochondrial dynamin related protein 1, a GTPase that regulates mitochondrial fission.[53] Bafilomycin A1 is a specific inhibitor for V-ATPase activity.[54] However, the treatment using either Mdivi-1 or bafilomycin A1 hardly reduced the cellular uptake of polymers (Figure 5b,c). Meanwhile, the side effect of dynasore is also reported to be related to reduced cellular cholesterol level and the dispersal of lipid raft.[50] From our previous results with MβCD-treatment for the uptake of four polymers in six different cell types

(Figure 2b, S6), the involvement of cell membrane cholesterol was shown to be minimal during the endocytosis of amphiphilic polymers. Treatment with nystatin, another cholesterol sequestering agent,[55] caused ~10–15% decrease for the cellular uptake of polymers (Figure 5d). The difference between MβCD- and nystatin-treatment could potentially be attributed to their different mechanisms of action, i.e. nystatin causes pore formation in lipid-based membranes (such as cell membrane) while MβCD does not.[56]

Actin and clathrin proteins are involved in the cellular uptake of amphiphilic polymers

The other major off-target effect of dynasore is related to the regulation of actin cytoskeleton, including cell shrinkage and suppression on lamellipodia formation.[46, 47, 57] Therefore, we employed a series of cytoskeletal drugs to screen their effect on the endocytosis of amphiphilic polymers. The cellular uptake of amphiphilic polymers was barely affected after the treatment of nocodazole (Figure 5e), an agent that disrupts cellular microtubules.[58] Next, the effect of actin polymerization inhibitors was evaluated on the cellular uptake of amphiphilic polymers. Cytochalasin[59] and latrunculin[60] analogs are representative agents that interfere actin polymerization. During the actin polymerization process, the globular actin monomers (G-actins) assemble into actin filaments (F-actin). Cytochalasin interferes the process by binding to the end of F-actin, preventing further addition of G-actin onto F-actin.[59] Latrunculin interrupts the process by irreversibly binding with G-actin, preventing G-actin from polymerization.[61]

In the cytochalasin analog, cytochalasin D[62] exhibited a universal ~20% inhibition on the cellular uptake of all polymers (Figure 5g). In the latrunculin analog, as a stronger actin binding agent (Figure 5j),[63] latrunculin A exhibited ~50% inhibition on the cellular uptake of all polymers (Figure 5h,k). In each analog, the weaker derivative (cytochalasin B and 16-epi-latrunculin B) did not affect the endocytosis of polymers bearing surface charge (Figure 5f,i). The inhibition results from cytoskeletal drugs confirms the involvement of actin during the endocytosis of amphiphilic polymers. Considering the reported side effect of dynasore on the actin of dynamin-triple knockout cells, including suppressing lamellipodia formation and stalling membrane ruffling,[47] it is reasonable to conclude that a major part of the off-target effects from dynasore was interfering the actin activity, thus reducing the cellular uptake of amphiphilic polymers.

The role of actin during polymer endocytosis was further evaluated by using genistein, an inhibitor for tyrosine kinase. The inhibition of genistein-sensitive tyrosine kinase has been reported to inhibit actin polymerization.[64] As expected, genistein-treatment inhibited more than 60% cellular uptake of **PEG** and **POS**. Meanwhile, the uptake of **NEG** and **MPC** was reduced by ~50% for **NEG** and ~40% for **MPC** after treating HeLa cells with 100 μM genistein (Figure 6a). The inhibition from genistein on the cellular uptake of **PEG** and **POS** was relatively higher than the effect of actin inhibitors, indicating that genistein may have affected other cellular components other than actin. In fact, genistein also interferes other processes that are dependent on tyrosine phosphorylation, such as the recruitment of scaffold proteins (e.g. epidermal growth factor receptor) into clathrin-coated pits.[65] To further understand this process, we evaluated the cellular uptake of amphiphilic polymers after treating cells with Pitstop 2, an inhibitor that interferes the terminal domain function of

clathrin and stalls the dynamics of clathrin-coated pits.[66] After Pitstop-2 treatment, about 40~50% inhibition of uptake was observed from **PEG** and **POS**, with ~20% inhibition on the uptake of **MPC** (Figure 6b). The uptake of **NEG** was not significantly affected by Pitstop-2 treatment, agreeing with the result from chlorpromazine treatment. The result suggests that the anionic polymers within our tested library is primarily endocytosed through macropinocytosis, with less contributions from the clathrin-mediated pathway than other polymers. Overall, actin and clathrin proteins are majorly involved during the cellular uptake of amphiphilic polymers.

Cellular uptake of amphiphilic polymers is majorly through macropinocytosis and clathrin-mediated endocytosis

The results so far suggest that the endocytosis of amphiphilic polymers with different surface charge is majorly contributed by micropinocytosis, with the involvement of the clathrin-mediated endocytosis for cationic and charge-neutral polymers (Figure 7). Although dynasore showed a dominant inhibition for the cellular uptake of amphiphilic polymers, the uptake of polymers was either increased or not affected when cellular dynamin was deficient. Meanwhile, other dynamin inhibitors with different mechanism of action did not affect the cellular uptake of polymers. Combining with the reported off-target effects of dynasore[50] and its binding capability with detergents,[44] we infer that the nearly diminished polymer uptake was not because of the inhibition on dynamin activity. During clathrin-mediated endocytosis, it is generally believed that dynamin is a scission protein during the formation of endocytic vesicles. However, when the forming endocytic vesicles separate from the cell membrane, other scission proteins (such as BAR proteins) are also involved in the process,[67] although the exact contribution of these proteins is not clear. In addition, the pulling force produced by actin polymerization facilitates the membrane fission in cooperation with the BAR proteins (e.g. endophilin 2).[46, 67] These components could possibly contribute to the increased cellular uptake of polymers that we observed in dynamin-deficient cells. Moreover, we have shown that actin is highly involved in the endocytosis of amphiphilic polymers by screening a series of pharmacological inhibitors (Figure 5,6). Considering that macropinocytosis is an actin-driven process,[68] we infer that actin is an essential protein for the endocytosis of amphiphilic polymers rather than dynamin (Figure 7). The cellular uptake increase of polymers in dynamin-deficient cells can be potentially attributed to the F-actin accumulation at clathrin-coated pits that was previously observed in dynamin-deficient cells.[46] As a result, macropinocytosis and clathrin-mediated endocytosis are two complementary processes that contribute to the uptake of amphiphilic polymers.

We summarized a series of recent reports regarding the effect of surface charge on the cellular entry of functional materials (Table S2). However, no general rules have been reached so far.[6, 69] Several factors have to be taken into account for the interaction between materials and biological systems, including the size, shape, surface area, roughness, porosity, functional groups, crystallinity, etc. of materials.[4] Surface charge indeed plays a role during the cellular uptake of functional materials. For example, in the current study, although sharing similar endocytic pathways, amphiphilic polymers with different surface charge exhibited different extent of cellular uptake (Figure S5). The effect of structural variations

on the cellular uptake of polymers is currently under investigations in our ongoing studies. Nonetheless, the methodological interplay on cellular uptake indeed ruled out possible misinterpretations such as the contribution of dynamins indicated by dynasore-treatment.

Conclusions

In summary, we have demonstrated an orthogonal end-group labeling strategy for amphiphilic polymers and evaluated the cellular uptake of amphiphilic polymers through the interplay of pharmacological and genetic approaches. The labelling strategy is applicable to synthetic polymers constructed through RAFT polymerization, ensuring the conjugation of one fluorophore on each polymer chain through click chemistry and allowing the investigation of their cellular uptake through simply tracking the tagged fluorophore. Moreover, our orthogonal labelling strategy presents a straightforward method to functionalize the end-group of polymer chains beyond fluorophore labeling, such as conjugation of organelle-targeting moieties or functional biomacromolecules. In a broader context, the robust end-group functionalization on polymers provides a versatile scaffold for the construction of precisely controlled supramolecular systems.

Next, the cellular uptake evaluation of these orthogonally labelled amphiphilic polymers leads to disagreement between pharmacological and genetic approaches regarding dynamin, an important protein involved in clathrin-mediated endocytosis. In detail, the cellular uptake of amphiphilic polymers was significantly reduced upon the treatment of dynasore, a potent dynamin inhibitor. However, the entry of amphiphilic polymers was upregulated in dynamin-deficient cells. The conflicting outcome between two approaches suggests the necessity of methodological interplay for probing the cellular uptake mechanism of materials of interest. The methodological interplay minimized the misinterpretation that can be generated by one methodology alone, revealing the role of actin rather than dynamin during the endocytosis of amphiphilic polymers. Our study reveals the importance of interplaying pharmacological and genetic approaches for the evaluation of cellular uptake mechanism, providing insights on elucidating the cellular uptake of next-generation therapeutics.

Supplementary Material

Refer to Web version on PubMed Central for supplementary material.

Acknowledgement

We thank the support from NIGMS of the National Institutes of Health (GM-065255). The authors thank Dr. James J. Chambers at the Light Microscopy Facility of the Institute for Applied Life Sciences (UMass Amherst) for providing valuable suggestions, and Dr. Mingxu You (UMass Amherst) for generously sharing the flow cytometer. We are grateful to receive gift cell lines from colleagues: RAW264.7 and HepG2 cell lines from Dr. Vincent M. Rotello (UMass Amherst), primary mouse embryo fibroblasts from Dr. Jesse Mager (UMass Amherst), DNM2-GFP SK-MEL-2 cell line from Dr. David G. Drubin (UC Berkeley), and conditional dynamin triple knockout mouse embryo fibroblasts from Dr. Pietro De Camilli (Yale).

References

1. Blanco E; Shen H; Ferrari M, Principles of nanoparticle design for overcoming biological barriers to drug delivery. Nat. Biotechnol 2015, 33, 941. [PubMed: 26348965]

2. Behzadi S; Serpooshan V; Tao W; Hamaly MA; Alkawareek MY; Dreaden EC; Brown D; Alkilany AM; Farokhzad OC; Mahmoudi M, Cellular uptake of nanoparticles: journey inside the cell. Chem. Soc. Rev 2017, 46 (14), 4218–4244. [PubMed: 28585944]

3. Hillaireau H; Couvreur P, Nanocarriers' entry into the cell: relevance to drug delivery. Cell. Mol. Life Sci 2009, 66 (17), 2873–2896. [PubMed: 19499185]

4. Nel AE; Mädler L; Velegol D; Xia T; Hoek EMV; Somasundaran P; Klaessig F; Castranova V; Thompson M, Understanding biophysicochemical interactions at the nano–bio interface. Nat. Mater 2009, 8, 543. [PubMed: 19525947]

5. Verma A; Stellacci F, Effect of Surface Properties on Nanoparticle–Cell Interactions. Small 2010, 6 (1), 12–21. [PubMed: 19844908]

6. Zhao F; Zhao Y; Liu Y; Chang X; Chen C; Zhao Y, Cellular Uptake, Intracellular Trafficking, and Cytotoxicity of Nanomaterials. Small 2011, 7 (10), 1322–1337. [PubMed: 21520409]

7. Ivanov AI, Pharmacological Inhibition of Endocytic Pathways: Is It Specific Enough to Be Useful? In Exocytosis and Endocytosis, Ivanov AI, Ed. Humana Press: Totowa, NJ, 2008; pp 15–33.

8. Iversen T-G; Skotland T; Sandvig K, Endocytosis and intracellular transport of nanoparticles: Present knowledge and need for future studies. Nano Today 2011, 6 (2), 176–185.

9. Dutta D; Donaldson JG, Search for inhibitors of endocytosis. Cell. Logist 2012, 2 (4), 203–208. [PubMed: 23538558]

10. Al Soraj M; He L; Peynshaert K; Cousaert J; Vercauteren D; Braeckmans K; De Smedt SC; Jones AT, siRNA and pharmacological inhibition of endocytic pathways to characterize the differential role of macropinocytosis and the actin cytoskeleton on cellular uptake of dextran and cationic cell penetrating peptides octaarginine (R8) and HIV-Tat. J. Controlled Release 2012, 161 (1), 132–141.

11. Ho LWC; Yung W-Y; Sy KHS; Li HY; Choi CKK; Leung KC-F; Lee TWY; Choi CHJ, Effect of Alkylation on the Cellular Uptake of Polyethylene Glycol-Coated Gold Nanoparticles. ACS Nano 2017, 11 (6), 6085–6101. [PubMed: 28562003]

12. Adams ML; Lavasanifar A; Kwon GS, Amphiphilic block copolymers for drug delivery. J. Pharm. Sci 2003, 92 (7), 1343–1355. [PubMed: 12820139]

13. Li L; Raghupathi K; Song C; Prasad P; Thayumanavan S, Self-assembly of random copolymers. Chem. Commun 2014, 50 (88), 13417–13432.

14. Torchilin VP, Targeted polymeric micelles for delivery of poorly soluble drugs. Cell. Mol. Life Sci 2004, 61 (19–20), 2549–2559. [PubMed: 15526161]

15. Onaca O; Enea R; Hughes DW; Meier W, Stimuli-Responsive Polymersomes as Nanocarriers for Drug and Gene Delivery. Macromol. Biosci 2009, 9 (2), 129–139. [PubMed: 19107717]

16. Bromberg LE; Ron ES, Temperature-responsive gels and thermogelling polymer matrices for protein and peptide delivery. Adv. Drug Del. Rev 1998, 31 (3), 197–221.

17. Zhou YF; Huang W; Liu JY; Zhu XY; Yan DY, Self-Assembly of Hyperbranched Polymers and Its Biomedical Applications. Adv. Mater 2010, 22 (41), 4567–4590. [PubMed: 20853374]

18. Yang X; Li Z; Wang N; Li L; Song L; He T; Sun L; Wang Z; Wu Q; Luo N; Yi C; Gong C, Curcumin-Encapsulated Polymeric Micelles Suppress the Development of Colon Cancer In Vitro and In Vivo. Sci. Rep 2015, 5, 10322. [PubMed: 25980982]

19. Luxenhofer R; Sahay G; Schulz A; Alakhova D; Bronich TK; Jordan R; Kabanov AV, Structure-property relationship in cytotoxicity and cell uptake of poly(2-oxazoline) amphiphiles. J. Controlled Release 2011, 153 (1), 73–82.

20. Robin MP; O'Reilly RK, Strategies for preparing fluorescently labelled polymer nanoparticles. Polym. Int 2015, 64 (2), 174–182.

21. Gordon MR; Zhao B; Anson F; Fernandez A; Singh K; Homyak C; Canakci M; Vachet RW; Thayumanavan S, Matrix Metalloproteinase-9-Responsive Nanogels for Proximal Surface Conversion and Activated Cellular Uptake. Biomacromolecules 2018, 19 (3), 860–871. [PubMed: 29360342]

22. Chiu Y-L; Ho Y-C; Chen Y-M; Peng S-F; Ke C-J; Chen K-J; Mi F-L; Sung H-W, The characteristics, cellular uptake and intracellular trafficking of nanoparticles made of hydrophobically-modified chitosan. J. Controlled Release 2010, 146 (1), 152–159.

23. Goda T; Goto Y; Ishihara K, Cell-penetrating macromolecules: Direct penetration of amphipathic phospholipid polymers across plasma membrane of living cells. Biomaterials 2010, 31 (8), 2380–2387. [PubMed: 20004016]
24. Wong C-H; Zimmerman SC, Orthogonality in organic, polymer, and supramolecular chemistry: from Merrifield to click chemistry. Chem. Commun 2013, 49 (17), 1679–1695.
25. Roth PJ; Wiss KT; Zentel R; Theato P, Synthesis of Reactive Telechelic Polymers Based on Pentafluorophenyl Esters. Macromolecules 2008, 41 (22), 8513–8519.
26. Zhu Y; Noy J-M; Lowe AB; Roth PJ, The synthesis and aqueous solution properties of sulfobutylbetaine (co)polymers: comparison of synthetic routes and tuneable upper critical solution temperatures. Polym. Chem 2015, 6 (31), 5705–5718.
27. Mangold SL; Carpenter RT; Kiessling LL, Synthesis of Fluorogenic Polymers for Visualizing Cellular Internalization. Org. Lett 2008, 10 (14), 2997–3000. [PubMed: 18563907]
28. Grassart A; Cheng AT; Hong SH; Zhang F; Zenzer N; Feng Y; Briner DM; Davis GD; Malkov D; Drubin DG, Actin and dynamin2 dynamics and interplay during clathrin-mediated endocytosis. J. Cell Biol 2014, 205 (5), 721–735. [PubMed: 24891602]
29. Chiefari J; Chong YK; Ercole F; Krstina J; Jeffery J; Le TPT; Mayadunne RTA; Meijs GF; Moad CL; Moad G; Rizzardo E; Thang SH, Living free-radical polymerization by reversible addition-fragmentation chain transfer: The RAFT process. Macromolecules 1998, 31 (16), 5559–5562.
30. Moad G; Rizzardo E; Thang SH, Living radical polymerization by the RAFT process. Aust. J. Chem 2005, 58 (6), 379–410.
31. Quémener D; Davis TP; Barner-Kowollik C; Stenzel MH, RAFT and click chemistry: A versatile approach to well-defined block copolymers. Chem. Commun 2006, 48, 5051–5053.
32. Krenske EH; Izgorodina EI; Coote ML, An Ab Initio Guide to Structure—Reactivity Trends in Reversible Addition Fragmentation Chain Transfer Polymerization. In Controlled/Living Radical Polymerization, American Chemical Society: 2006; Vol. 944, pp 406–420.
33. Yang J; Luo K; Pan H; Kopečková P; Kopeček J, Synthesis of biodegradable multiblock copolymers by click coupling of RAFT-generated heterotelechelic polyHPMA conjugates. React. Funct. Polym 2011, 71 (3), 294–302. [PubMed: 21499527]
34. Keddie DJ; Moad G; Rizzardo E; Thang SH, RAFT Agent Design and Synthesis. Macromolecules 2012, 45 (13), 5321–5342.
35. Soo Choi H; Liu W; Misra P; Tanaka E; Zimmer JP; Itty Ipe B; Bawendi MG; Frangioni JV, Renal clearance of quantum dots. Nat. Biotechnol 2007, 25, 1165. [PubMed: 17891134]
36. Jewett JC; Sletten EM; Bertozzi CR, Rapid Cu-Free Click Chemistry with Readily Synthesized Biarylazacyclooctynones. J. Am. Chem. Soc 2010, 132 (11), 3688–3690. [PubMed: 20187640]
37. Lu J; Liong M; Sherman S; Xia T; Kovochich M; Nel AE; Zink JI; Tamanoi F, Mesoporous Silica Nanoparticles for Cancer Therapy: Energy-Dependent Cellular Uptake and Delivery of Paclitaxel to Cancer Cells. NanoBiotechnology 2007, 3 (2), 89–95. [PubMed: 19936038]
38. Kim J-S; Yoon T-J; Yu K-N; Noh MS; Woo M; Kim B-G; Lee K-H; Sohn B-H; Park S-B; Lee J-K; Cho M-H, Cellular uptake of magnetic nanoparticle is mediated through energy-dependent endocytosis in A549 cells. J. Vet. Sci 2006, 7 (4), 321–326. [PubMed: 17106221]
39. Koivusalo M; Welch C; Hayashi H; Scott CC; Kim M; Alexander T; Touret N; Hahn KM; Grinstein S, Amiloride inhibits macropinocytosis by lowering submembranous pH and preventing Rac1 and Cdc42 signaling. J. Cell Biol 2010, 188 (4), 547–563. [PubMed: 20156964]
40. Zidovetzki R; Levitan I, Use of cyclodextrins to manipulate plasma membrane cholesterol content: Evidence, misconceptions and control strategies. Biochim. Biophys. Acta 2007, 1768 (6), 1311–1324. [PubMed: 17493580]
41. Kuhn DA; Vanhecke D; Michen B; Blank F; Gehr P; Petri-Fink A; Rothen-Rutishauser B, Different endocytotic uptake mechanisms for nanoparticles in epithelial cells and macrophages. Beilstein J. Nanotechnol 2014, 5, 1625–1636. [PubMed: 25383275]
42. Macia E; Ehrlich M; Massol R; Boucrot E; Brunner C; Kirchhausen T, Dynasore, a Cell-Permeable Inhibitor of Dynamin. Dev. Cell 2006, 10 (6), 839–850. [PubMed: 16740485]
43. Patel PC; Giljohann DA; Daniel WL; Zheng D; Prigodich AE; Mirkin CA, Scavenger Receptors Mediate Cellular Uptake of Polyvalent Oligonucleotide-Functionalized Gold Nanoparticles. Bioconjugate Chem. 2010, 21 (12), 2250–2256.

44. McCluskey A; Daniel JA; Hadzic G; Chau N; Clayton EL; Mariana A; Whiting A; Gorgani NN; Lloyd J; Quan A; Moshkanbaryans L; Krishnan S; Perera S; Chircop M; von Kleist L; McGeachie AB; Howes MT; Parton RG; Campbell M; Sakoff JA; Wang X; Sun J-Y; Robertson MJ; Deane FM; Nguyen TH; Meunier FA; Cousin MA; Robinson PJ, Building a Better Dynasore: The Dyngo Compounds Potently Inhibit Dynamin and Endocytosis. Traffic 2013, 14 (12), 1272–1289. [PubMed: 24025110]
45. Jimah JR; Hinshaw JE, Structural Insights into the Mechanism of Dynamin Superfamily Proteins. Trends Cell Biol. 2019, 29 (3), 257–273. [PubMed: 30527453]
46. Ferguson S; Raimondi A; Paradise S; Shen H; Mesaki K; Ferguson A; Destaing O; Ko G; Takasaki J; Cremona O; O' Toole E; De Camilli P, Coordinated Actions of Actin and BAR Proteins Upstream of Dynamin at Endocytic Clathrin-Coated Pits. Dev. Cell 2009, 17 (6), 811–822. [PubMed: 20059951]
47. Park RJ; Shen H; Liu L; Liu X; Ferguson SM; De Camilli P, Dynamin triple knockout cells reveal off target effects of commonly used dynamin inhibitors. J. Cell Sci 2013, 126 (22), 5305–5312. [PubMed: 24046449]
48. Quan A; McGeachie AB; Keating DJ; van Dam EM; Rusak J; Chau N; Malladi CS; Chen C; McCluskey A; Cousin MA; Robinson PJ, Myristyl Trimethyl Ammonium Bromide and Octadecyl Trimethyl Ammonium Bromide Are Surface-Active Small Molecule Dynamin Inhibitors that Block Endocytosis Mediated by Dynamin I or Dynamin II. Mol. Pharmacol 2007, 72 (6), 1425–1439. [PubMed: 17702890]
49. Hill TA; Gordon CP; McGeachie AB; Venn-Brown B; Odell LR; Chau N; Quan A; Mariana A; Sakoff JA; Chircop M; Robinson PJ; McCluskey A, Inhibition of Dynamin Mediated Endocytosis by the Dynoles—Synthesis and Functional Activity of a Family of Indoles. J. Med. Chem 2009, 52 (12), 3762–3773. [PubMed: 19459681]
50. Preta G; Cronin JG; Sheldon IM, Dynasore - not just a dynamin inhibitor. Cell Commun. Signal 2015, 13 (1), 24. [PubMed: 25889964]
51. Sakai H; Moriura Y; Notomi T; Kawawaki J; Ohnishi K; Kuno M, Phospholipase C-dependent Ca2+-sensing pathways leading to endocytosis and inhibition of the plasma membrane vacuolar H +-ATPase in osteoclasts. Am. J. Physiol. Cell Physiol 2010, 299 (3), C570–C578. [PubMed: 20592242]
52. Kozik P; Hodson NA; Sahlender DA; Simecek N; Soromani C; Wu J; Collinson LM; Robinson MS, A human genome-wide screen for regulators of clathrin-coated vesicle formation reveals an unexpected role for the V-ATPase. Nat. Cell Biol 2012, 15, 50.
53. Cassidy-Stone A; Chipuk JE; Ingerman E; Song C; Yoo C; Kuwana T; Kurth MJ; Shaw JT; Hinshaw JE; Green DR; Nunnari J, Chemical Inhibition of the Mitochondrial Division Dynamin Reveals Its Role in Bax/Bak-Dependent Mitochondrial Outer Membrane Permeabilization. Dev. Cell 2008, 14 (2), 193–204. [PubMed: 18267088]
54. Harada M; Sakisaka S; Yoshitake M; Kin M; Ohishi M; Shakado S; Mimura Y; Noguchi K; Sata M; Tanikawa K, Bafilomycin A1, a specific inhibitor of vacuolar-type H+-ATPases, inhibits the receptor-mediated endocytosis of asialoglycoproteins in isolated rat hepatocytes. J. Hepatol 1996, 24 (5), 594–603. [PubMed: 8773916]
55. Rothberg KG; Heuser JE; Donzell WC; Ying Y-S; Glenney JR; Anderson RGW, Caveolin, a protein component of caveolae membrane coats. Cell 1992, 68 (4), 673–682. [PubMed: 1739974]
56. Valitova J; Sulkarnayeva A; Kotlova E; Ponomareva A; Mukhitova FK; Murtazina L; Ryzhkina I; Beckett R; Minibayeva F, Sterol binding by methyl-β-cyclodextrin and nystatin – comparative analysis of biochemical and physiological consequences for plants. FEBS J. 2014, 281 (8), 2051–2060. [PubMed: 24612537]
57. Yamada H; Abe T; Li S-A; Masuoka Y; Isoda M; Watanabe M; Nasu Y; Kumon H; Asai A; Takei K, Dynasore, a dynamin inhibitor, suppresses lamellipodia formation and cancer cell invasion by destabilizing actin filaments. Biochem. Biophys. Res. Commun 2009, 390 (4), 1142–1148. [PubMed: 19857461]
58. Wang T-H; Wang H-S; Ichijo H; Giannakakou P; Foster JS; Fojo T; Wimalasena J, Microtubule-interfering Agents Activate c-Jun N-terminal Kinase/Stress-activated Protein Kinase through Both Ras and Apoptosis Signal-regulating Kinase Pathways. J. Biol. Chem 1998, 273 (9), 4928–4936. [PubMed: 9478937]

59. Matthew T, Using Cytochalasins to Improve Current Chemotherapeutic Approaches. Anti-Cancer Agents Med. Chem 2015, 15 (3), 327–335.

60. Morton WM; Ayscough KR; McLaughlin PJ, Latrunculin alters the actin-monomer subunit interface to prevent polymerization. Nat. Cell Biol 2000, 2, 376. [PubMed: 10854330]

61. Fujiwara I; Zweifel ME; Courtemanche N; Pollard TD, Latrunculin A Accelerates Actin Filament Depolymerization in Addition to Sequestering Actin Monomers. Curr. Biol 2018, 28 (19), 3183–3192.e3182. [PubMed: 30270183]

62. Sampath P; Pollard TD, Effects of cytochalasin, phalloidin and pH on the elongation of actin filaments. Biochemistry 1991, 30 (7), 1973–1980. [PubMed: 1899622]

63. Fürstner A; Kirk D; Fenster MDB; Aïssa C; De Souza D; Müller O, Diverted total synthesis: Preparation of a focused library of latrunculin analogues and evaluation of their actin-binding properties. Proc. Natl. Acad. Sci. U.S.A 2005, 102 (23), 8103–8108. [PubMed: 15917332]

64. Han SI; Ha K-S; Kang KI; Kim HD; Kang HS, Heat shock-induced actin polymerization, SAPK/JNK activation, and heat-shock protein expression are mediated by genistein-sensitive tyrosine kinase(s) in K562 cells. Cell Biol. Int 2000, 24 (7), 447–457. [PubMed: 10875892]

65. Sorkina T; Huang F; Beguinot L; Sorkin A, Effect of Tyrosine Kinase Inhibitors on Clathrin-coated Pit Recruitment and Internalization of Epidermal Growth Factor Receptor. J. Biol. Chem 2002, 277 (30), 27433–27441. [PubMed: 12021271]

66. von Kleist L; Stahlschmidt W; Bulut H; Gromova K; Puchkov D; Robertson Mark J.; MacGregor Kylie A.; Tomilin N; Pechstein A; Chau N; Chircop M; Sakoff J; Peter von Kries J; Saenger W; Kräusslich H-G; Shupliakov O; Robinson Phillip J.; McCluskey A; Haucke V, Role of the Clathrin Terminal Domain in Regulating Coated Pit Dynamics Revealed by Small Molecule Inhibition. Cell 2011, 146 (5), 841.

67. Kaksonen M; Roux A, Mechanisms of clathrin-mediated endocytosis. Nat. Rev. Mol. Cell Biol 2018, 19, 313. [PubMed: 29410531]

68. Bloomfield G; Kay RR, Uses and abuses of macropinocytosis. J. Cell Sci 2016, 129 (14), 2697–2705. [PubMed: 27352861]

69. Frohlich E, The role of surface charge in cellular uptake and cytotoxicity of medical nanoparticles. Int. J. Nanomed 2012, 7, 5577–5591.

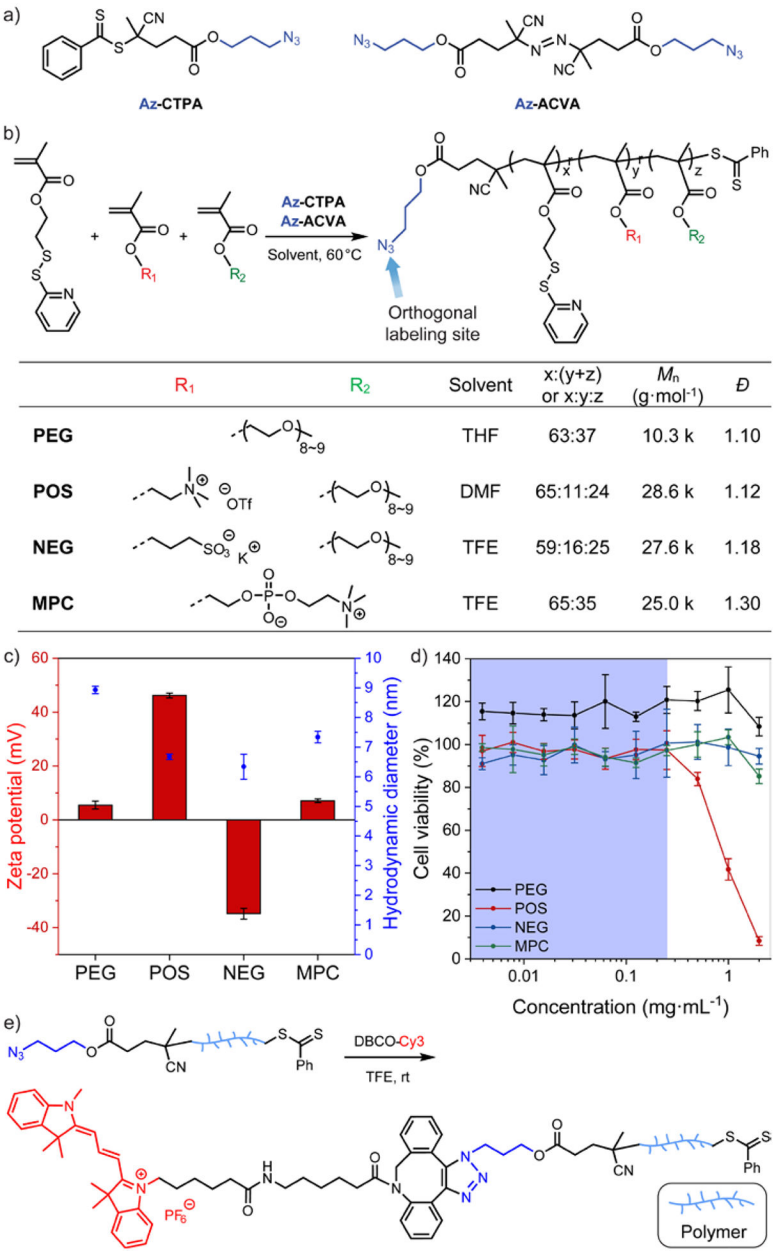

	R_1	R_2	Solvent	x:(y+z) or x:y:z	M_n (g·mol^{-1})	$Đ$
PEG			THF	63:37	10.3 k	1.10
POS			DMF	65:11:24	28.6 k	1.12
NEG			TFE	59:16:25	27.6 k	1.18
MPC			TFE	65:35	25.0 k	1.30

Figure 1.

(a) Chemical structure of the azido-derivative of chain transfer agent (Az-CTPA) and radical initiator (Az-ACVA) for RAFT polymerization. (b) Synthetic scheme and characterization of the amphiphilic polymer library. (c) Zeta potential and hydrodynamic diameter of the amphiphilic polymers. $N = 3$. The amphiphilic polymers were formulated with 10 mol% (vs. PDS units) of dithiothreitol to form the polymeric assemblies. (d) HeLa cell viability evaluation with amphiphilic polymers at different dosage. $N = 4$. In each figure, error bars represent the standard deviation of replicates. (e) Synthetic scheme of the orthogonal end-group labeling strategy for amphiphilic polymers.

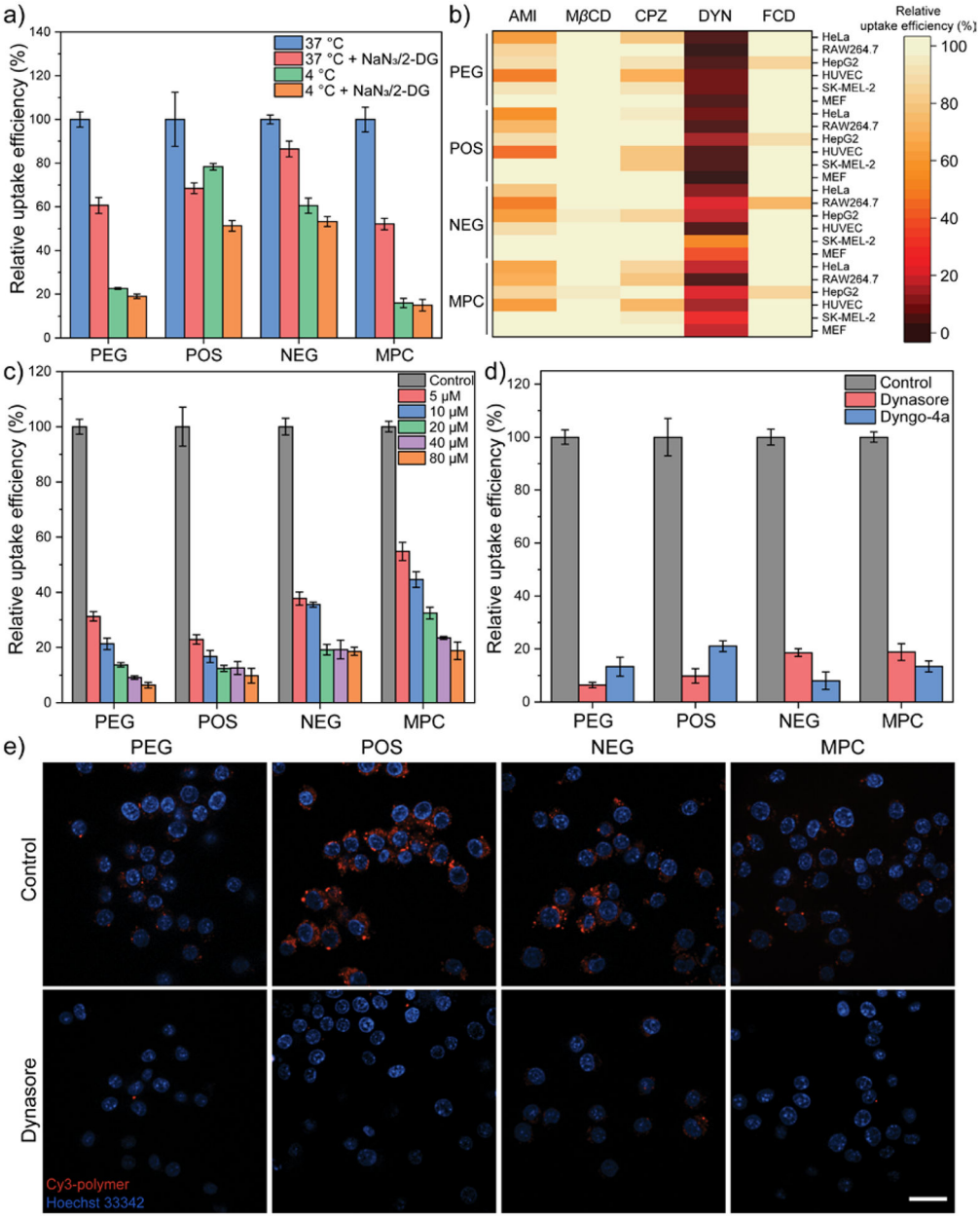

Figure 2.

(a) Cellular uptake efficiency of amphiphilic polymers after 3 hours in HeLa cells at low temperature and ATP depletion conditions (NaN_3/2-DG treatment). $N = 4$. 2-DG, 2-deoxy-D-glucose. (b) Cellular uptake efficiency of amphiphilic polymers after 3 hours in the presence of pharmacological inhibitors. The evaluation was performed in six different types of cell: HeLa, RAW264.7, HepG2, HUVEC, SK-MEL-2, and MEF. Each data was collected from the mean value of four replicates. AMI, amiloride. MβCD, methyl-β-cyclodextrin. CPZ, chlorpromazine. DYN, dynasore. FCD, fucoidan. (c) Cellular uptake efficiency of amphiphilic polymers after 3 hours in HeLa cells upon the treatment of different dynasore dosage. $N = 4$. (d) Comparison of dynasore and Dyngo-4a on the cellular uptake efficiency of amphiphilic polymers in HeLa cells. $N = 4$. (e) Confocal microscopic images of Cy3-

labelled amphiphilic polymers in RAW264.7 cells with or without the presence of dynasore. The scale bar in each figure represents 20 μm. In each figure, error bars represent the standard deviation of replicates.

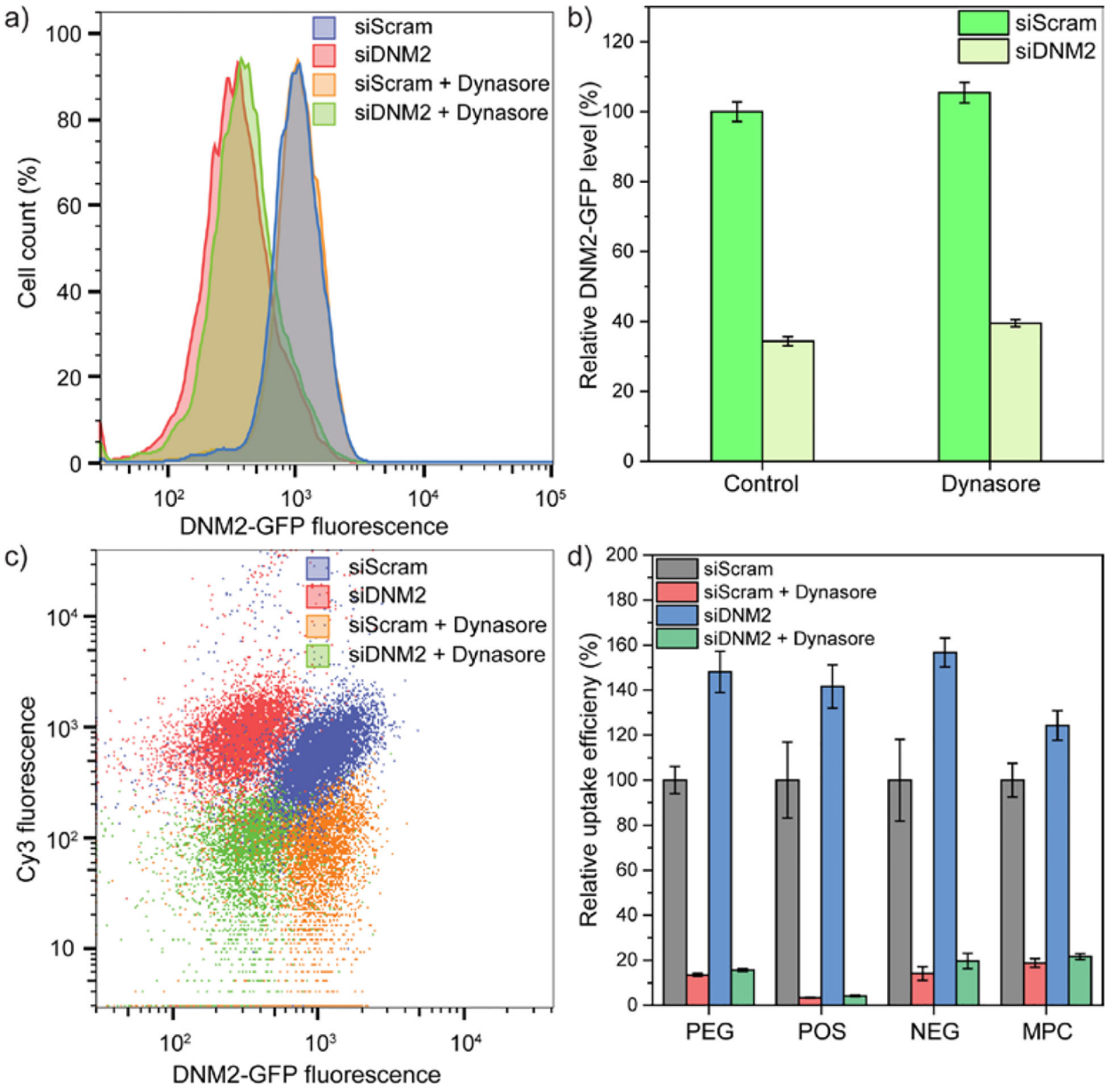

Figure 3.

(a) Representative histogram plot of green fluorescent protein (GFP) fluorescence intensity for DNM2-GFP SK-MEL-2 cells. Cells were treated with either scrambled siRNA or siRNA of dynamin-2 for 72 hours, with or without the subsequent treatment using dynasore. (b) Relative level of DNM2-GFP expression in SK-MEL-2 cells. The GFP intensity of scrambled siRNA-treated cells without subsequent dynasore treatment was normalized as 100%. $N = 16$. (c) Representative flow cytometry dot plots with GFP representing dynamin-2 expression on the x axis and Cy3 representing the cellular uptake of amphiphilic polymers on the y axis. A representative dataset from **PEG** was used as an example. (d) Cellular uptake efficiency of amphiphilic polymers after 3 hours in SK-MEL-2 cells. The cellular uptake intensity of polymers (Cy3 intensity) in scrambled siRNA-treated cells

without subsequent dynasore treatment was normalized as 100%. $N = 4$. In each figure, error bars represent the standard deviation of replicates.

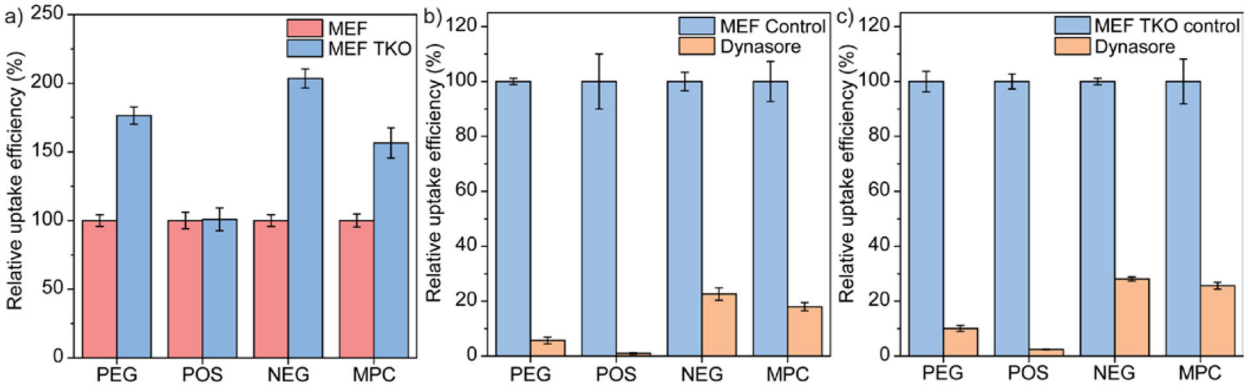

Figure 4.

(a) Cellular uptake efficiency of amphiphilic polymers after 3 hours in dynamin triple knockout mouse embryo fibroblasts (MEF TKO). The cellular uptake intensity of polymers (Cy3 intensity) in wild-type mouse embryo fibroblasts (MEF) were normalized as 100%. N = 4. (b) Cellular uptake efficiency of amphiphilic polymers after 3 hours in wild-type mouse embryo fibroblasts in the presence of dynasore. N = 4. (c) Cellular uptake efficiency of amphiphilic polymers after 3 hours in dynamin triple knockout mouse embryo fibroblasts in the presence of dynasore. N = 4. In each figure, error bars represent the standard deviation of replicates.

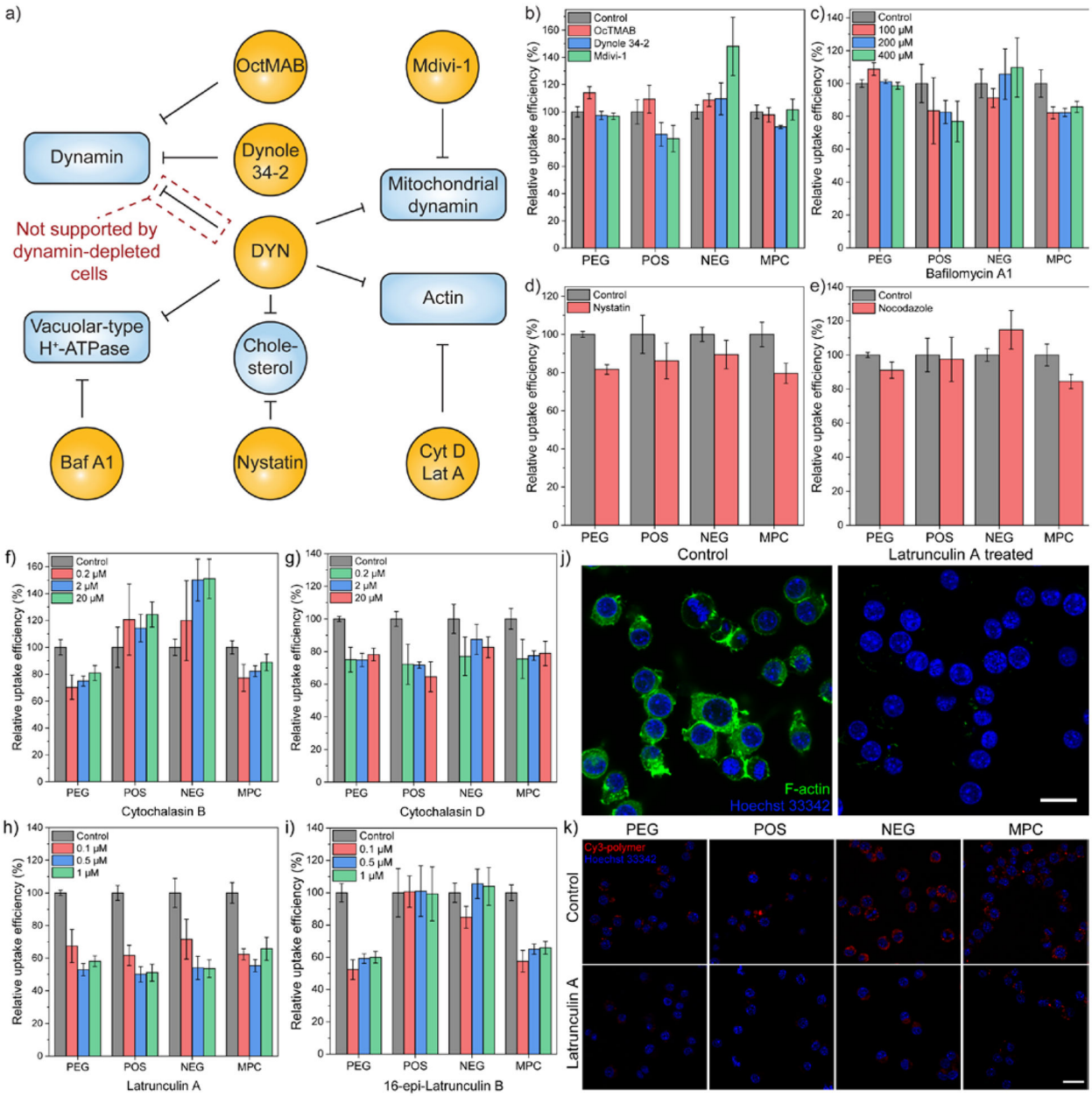

Figure 5.

(a) Workflow for screening the off-target effects of dynasore (DYN) on the cellular uptake of amphiphilic polymers. Baf A1, bafilomycin A1. Cyt D, cytochalasin D. Lat A, latrunculin A. OcTMAB, octadecyltrimethylammonium bromide. (b) Cellular uptake efficiency of amphiphilic polymers in HeLa cells in the presence of dynamin inhibitors, including OcTMAB, Dynole 34–2, and a mitochondrial dynamin inhibitor, Mdivi-1. (c) Cellular uptake efficiency of amphiphilic polymers after 3 hours in HeLa cells in the presence of bafilomycin A1, an inhibitor for vacuolar-type H^+-ATPase. $N = 4$. (d) Cellular uptake efficiency of amphiphilic polymers after 3 hours in HeLa cells in the presence of nystatin, a cholesterol-sequestration agent. $N = 4$. (e) Cellular uptake efficiency of amphiphilic polymers after 3 hours in HeLa cells in the presence of nocodazole, a microtubule-disruption

agent. (f~i) Cellular uptake efficiency of amphiphilic polymers after 30 minutes in HeLa cells in the presence of actin inhibitors, including (f) cytochalasin B, (g) cytochalasin D, (h) latrunculin A, (i) 16-epi-latrunculin B. $N = 4$. In each figure, error bars represent the standard deviation of replicates. (j) Actin filament staining in RAW264.7 cells before and after latrunculin A treatment. Treated RAW264.7 cells were fixed and stained with phalloidin-iFluor 488 reagent. (k) Confocal microscopic images of Cy3-labelled amphiphilic polymers in RAW264.7 cells with or without the presence of latrunculin A. The scale bar in each figure represents 20 μm. In each figure, error bars represent the standard deviation of replicates.

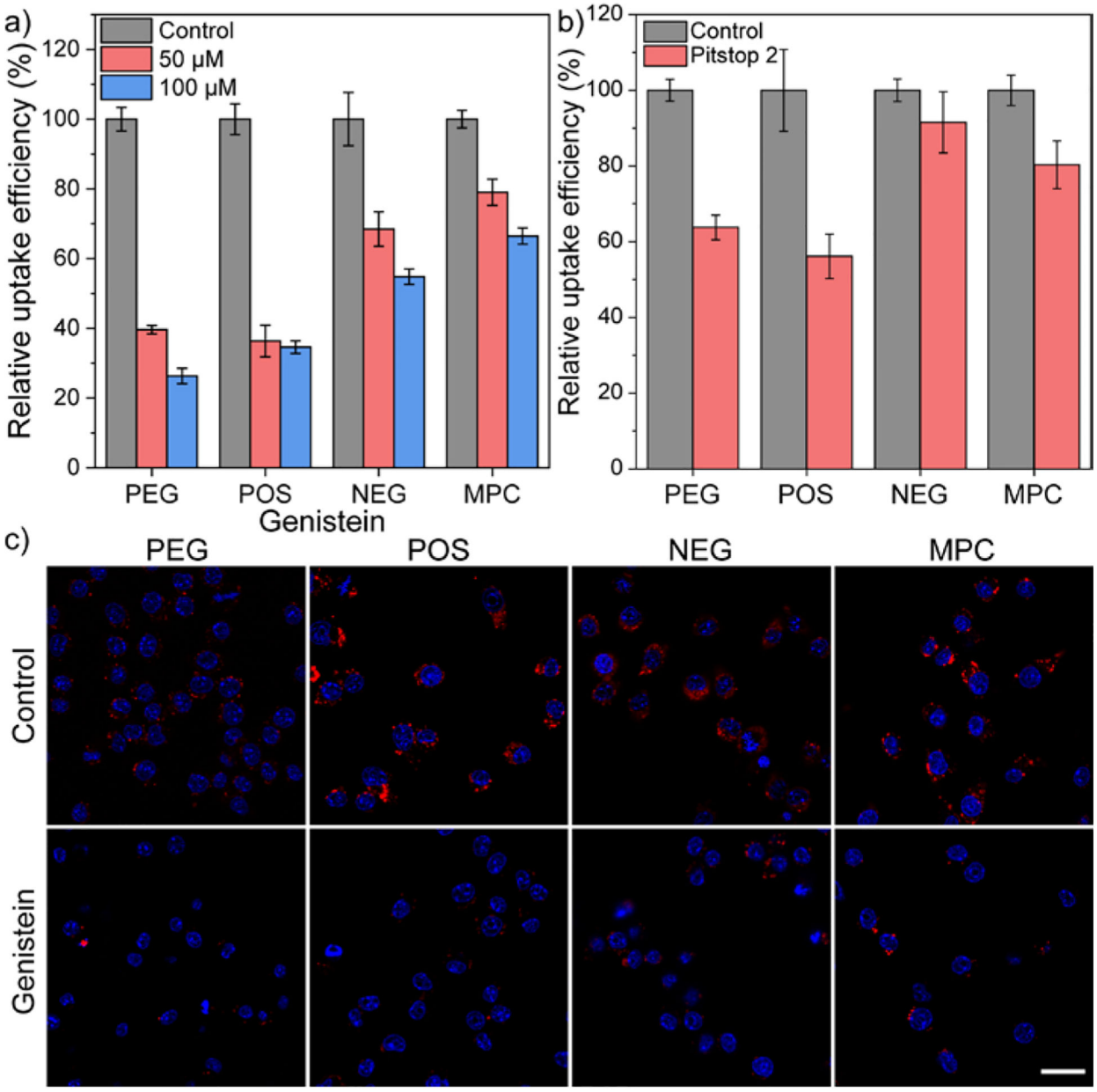

Figure 6.

(a) Cellular uptake efficiency of amphiphilic polymers after 3 hours in HeLa cells in the presence of genistein, an inhibitor for tyrosine kinase. $N = 4$. (b) Cellular uptake efficiency of amphiphilic polymers after 3 hours in HeLa cells in the presence of Pitstop 2, a cell-permeable clathrin inhibitor. $N = 4$. In each figure, error bars represent the standard deviation of replicates. (c) Confocal microscopic images of Cy3-labelled amphiphilic polymers in RAW264.7 cells with or without the presence of 100 μM genistein. The scale bar in each figure represents 20 μm.

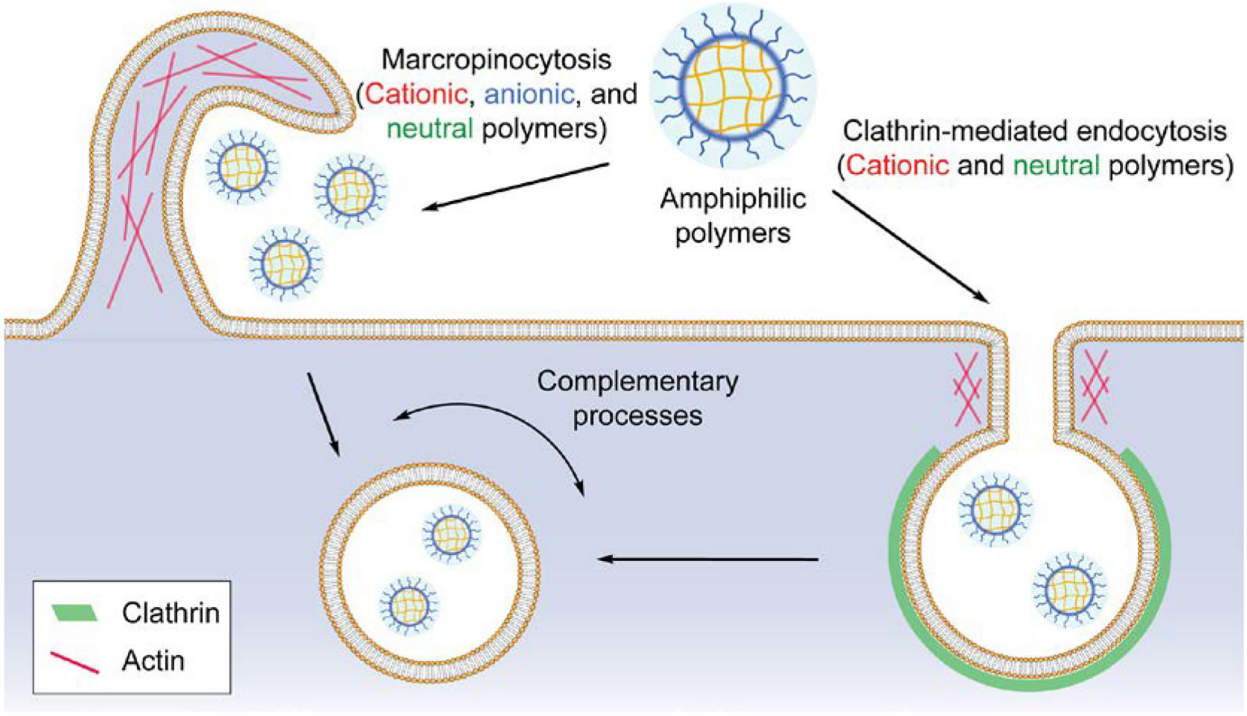

Figure 7.
Model for the cellular uptake process of amphiphilic polymers.